Aqueous-sensitive reaction sites in sulfonic acid-functionalized mesoporous silicas

Gabriel Morales,[‡] George Athens,[§] Bradley F. Chmelka,[§] Rafael van Grieken,[‡] and Juan A. Melero,[‡*]

[§] Department of Chemical Engineering, University of California, Santa Barbara, California 93106 U.S.A.

[‡] Department of Chemical and Environmental Technology, ESCET, Rey Juan Carlos University, C/ Tulipán s/n, 28933, Móstoles (Madrid), Spain.

Published on:
Journal of Catalysis 254 (2008) 205-217
doi:10.1016/j.jcat.2007.12.011

* To whom correspondence should be addressed

e-mail address: juan.melero@urjc.es

Abstract

Local differences in surface hydrophilicities/hydrophobicities of propyl- and arene-sulfonic-acid modified mesoporous silica and organosilica catalysts have been compared and correlated with their bulk catalytic properties for aqueous-sensitive organic reactions. Syntheses of propyl- and arene-SO_3H-modified mesoporous silicas and organosilicas yield materials with different hydrophilicities, especially when ethylsiloxane moieties are incorporated into the silica frameworks. Solid-state two-dimensional (2D) $^{13}C\{^1H\}$ and $^{29}Si\{^1H\}$ heteronuclear correlation (HETCOR) NMR spectra prove that the incorporation of hydrophobic ethylsiloxane groups into functionalized mesoporous silica frameworks result in reduced interactions of adsorbed water with the silica framework in general and, importantly, in the immediate vicinities of the SO_3H active sites. The hydrophilic/hydrophobic character of the surface, as well as the active site properties depend on the functional species attached. Propyl-sulfonic acid moieties are less acidic but more hydrophobic than arene-SO_3H species, leading to superior overall activities for water-mediated acid-catalyzed organic reactions. The etherification of vanillyl alcohol (4-hydroxy-3-methoxybenzylalcohol) with 1-hexanol to yield 4-hydroxy-3-methoxybenzyl-1-hexyl ether is shown to proceed significantly more effectively on SO_3H-modified mesoporous organosilicas, compared to wholly siliceous mesoporous supports. The correlation of macroscopic adsorption and reaction results with 2D NMR measurements allows the hydrophilic/hydrophobic surface properties of the mesoporous support to be optimized with respect to water-retention capacities and activities for water-sensitive organic reactions.

Keywords: mesostructured silica, mesoporous organosilica, surface hydrophobicity, etherification, benzyl alcohol, sulfonic acid, 2D NMR.

1. Introduction

The development of heterogeneous catalysts to replace homogeneous systems for the production of fine chemicals is motivated by several potential process improvements [1-2]. These include easier separation of the catalyst from the reaction medium, greater catalyst stability, improved regenerability, and enhanced product selectivity, when the active sites are attached to a solid surface, typically within high-surface-area porous materials. Likewise, tightening environmental regulation of traditional acid-catalyzed chemical processes (alkylation, acylation, isomerization, oligomerization, etc) has provided an opportunity for new solid-acid catalysts to replace strong liquid acids [3-4].

However, to achieve the combination or even a subset of the process advantages that heterogeneous catalysts may permit, numerous materials challenges must be overcome. These include mitigating or exploiting the effects of reduced active site mobility, lower entropy, confinement, diffusion limitations to mass transport, and competitive adsorption at nearby surface sites. Heterogeneous acid catalysts for fine chemical syntheses face all of these issues and, in particular the latter, because of the difficulty in managing the inherent amphiphilicity of the organo-acid functional species. The relative incompatibilities of the hydrophilic acid sites, their accompanying hydrophobic organic links to the support, and their interactions with the organic reactants and products of interest tend to be exacerbated when attached to solid surfaces.

Such heterogenized catalysts are often based on porous silica supports, primarily because of their high surface areas and porosities, excellent stabilities (chemical and thermal), and facile functionalization with catalytically active organic groups with catalytic activity that can be robustly anchored to the support surfaces. Mesostructured silica materials are particularly promising as supports for active species, due to their very high surface areas (>800 m^2/g), large pores (2-50 nm) for low diffusional

resistances to mass transport, and adjustable and narrow pore size distributions with high active-site accessibilities [5-7]. A number of recent studies, including our own, have reported the incorporation of sulfonic-acid groups into mesostructured pore channels of MCM-41, HMS, or SBA-type materials [8-15] to introduce acid-catalysis or ion-conducting properties. Such properties, can furthermore be modified by different moieties adjacent to the sulfonic-acid site, such as arene-sulfonic [13] or perfluorosulfonic groups [15-17], whose electron-withdrawing characters lead to enhanced acidity. Efforts to maximize the hydrophobicity [18] or hydrophilicity [15] in the near vicinities of the sulfonic-acid sites are enabling new applications for these materials. For example, sulfonic-acid functionalized mesoporous silicas have been shown to have improved reaction properties over conventional homogeneous or heterogeneous catalysts for a wide range of acid-catalyzed reactions, including esterification [12, 19-21], condensation and addition [9, 22-23], etherification [24], rearrangement [25-27], Friedel-Crafts acylation [28] , alkylation [27] and conversion of biorenewable molecules [29-30]. Recently they have also shown enhanced proton-conductivities [15].

The anchoring of organic acid moieties to mesoporous silica surfaces by covalent bonds has generally followed two protocols, either post-synthetic grafting of the acid species to accessible pore surfaces after the silica framework has been formed or co-condensation of the acid functional species simultaneously as the silica framework cross-links. Post-synthesis grafting methods are based primarily on the reaction of organosilanes ($(R'O)_3SiR$) or chlorosilanes (Cl_3SiR) with silanol groups on the interior mesopore channels of previously synthesized (e.g., self-assembled and then calcined or extracted) mesoporous silica. This functionalization approach allows for a wide range of organic species to be anchored to the silica surface without affecting the mesostructural

ordering of the separately prepared mesoporous silica support. Furthermore, the versatile processability of mesostructured block-copolymer-directed silica permits facile control over particle or bulk morphologies and separate surface incorporation of multiple functional species into the mesoporous silica. However, grafting techniques often lead to rather low loading of functional groups and/or require the use of multiple separate processing steps. Hence, there is interest in the incorporation of relatively high functional groups loadings by single-step co-assembly processes.

Co-condensation (frequently referred to also as “one-pot syntheses”) involves the simultaneous condensation of tetra-alkoxysilanes ($(RO)_4Si$) with terminal tri-alkoxyorganosilanes $(RO)_3SiR'$, where R’ can be a sulfonic-acid-containing organic moiety in the presence of a structure-directing surfactant agent, yielding mesostructured organically-modified silica [11,13]. The incorporation of the acidic functional species occurs in a single process step, after which the surfactant species are removed to produce the porosity needed to allow access to the acid sites in the mesopore channels. High concentrations of the acid precursor species tend to disrupt mesostructural ordering and make it difficult to control bulk morphologies (e.g., particle, film, fiber, or monolith). For powders used in catalytic applications, however, these challenges are less troublesome, and moreover, higher and more uniform surface concentrations of acid-centers have been achieved using co-condensation strategies, which, when suitable, are often more convenient than post-synthetic grafting approaches.

In particular, a co-condensed, ‘one-pot’ synthesis protocol of mesoporous solid-acid catalysts with hybrid organosilica frameworks allows for substantial control of local hydrophobic/hydrophilic environments near the active site. This strategy relies on the co-condensation of hydrolyzed trialkoxyorganosilanes of the type $(R'O)_3Si\text{-}R\text{-}Si(OR')_3$, where the bridging moiety, -R-, can be composed of various organic groups (e.g.,

ethane, benzene, thiophene, or biphenylene) [31-34], in what have been referred to as 'periodic mesoporous organosilicas' (PMOs). These materials combine several advantageous aspects of both organic and inorganic species into mesoporous solids with mechanical, adsorption, and reaction properties that are different from either of the wholly organic or inorganic components. Furthermore, recent work has shown improved catalytic performance of sulfonic-acid active sites supported on mesoporous organosilica in water-sensitive reactions [20,35-37]. The higher catalytic activity of these materials has been attributed to increased hydrophobicity near the sulfonic-acid moieties and enhanced diffusion of reactant and products within the hydrophobic mesopores**.**

Thus, interactions among the -SO_3H groups, adjacent moieties (including framework and grafted species) and water molecules are important to elucidate and control. A number of different techniques have been employed to investigate structural properties, acid capacities, organic incorporation, oxidation efficiencies and acid strength of these sulfonic acid modified mesostructured materials. Furthermore, advanced 2D solid-state NMR spectroscopy techniques have been shown to be powerful tools to characterize and identify sites, species and interactions in mesostructured materials [38]. Recently, Trebosc et al. [39] reported the utilization of high resolution solid-state 2D heteronuclear correlation (HETCOR) NMR spectroscopy under fast magic angle spinning to provide highly resolved spectra between protons and low-gamma nuclei (^{13}C and ^{29}Si) in allyl-functionalized MCM-41 samples. These methods provide detailed structural characterization of surfaces of mesoporous solid and herein they are applied for the first time to sulfonic acid-modified silica and organosilica materials. Specifically, interactions among the different ^{29}Si, ^{13}C and ^{1}H species have been examined to obtain surface-structure correlations with catalytic reaction properties.

These are expected to be important especially when highly polar molecules (e.g. water molecules) are present in the reaction medium. We demonstrate how control of molecular surface hydrophilicity or hydrophobicity in propyl- and arene-sulfonic acid-modified PMO materials can influence the etherification of vanillyl alcohol, a bulky benzyl alcohol, in the presence of 1-hexanol, which react to yield 4-hydroxy-3-methoxybenzyl cyclohexyl ether, a representative fine chemical compounds used in perfumes and flavorings.

2. Experimental

2.1 Catalyst preparation

Propyl-sulfonic-acid functionalized mesostructured silica and organosilica were synthesized following a one-pot co-condensation procedure previously employed for the preparation of propyl-sulfonic-acid functionalized silica SBA-15 [11]. For the case of the organosilica, 1,2-*bis*-(triethoxysilyl)ethane (BTSE, Aldrich) was additionally incorporated. In a typical synthesis, 4 g of poly(alkylene oxide) triblock copolymer ($EO_{20}PO_{70}EO_{20}$) (Aldrich) were dissolved in 125 mL of 1.9 M HCl. The solution was heated to 40 ^{o}C and then tetraethoxysilane (TEOS, Aldrich), or a mixture of TEOS and BTSE in the desired ratio, was added, after which the mixture was allowed to prehydrolyze for 45 min. Then mercapto-propyltrimethoxysilane (MPTMS, Aldrich) and an aqueous solution of H_2O_2 (30 wt%, Merck) were added at once. The mixture was stirred vigorously at 40 ^{o}C for 20 h and then aged at 100 ^{o}C for 24 h under static conditions. Solid products were recovered by filtration and air-dried overnight. The block copolymer species were subsequently removed by ethanol washing under reflux for 24 h (2 g of as-synthesized material per 200 mL of ethanol). Molar composition of the mixtures, relative to 4 g of triblock copolymer, were: (0.0369 - *x*) TEOS: (*x*/2)

BTSE: (0.0041) MPTMS: (0.0369) H_2O_2: 0.24 HCl: ≈ 6.67 H_2O, with *x* being either 0 or 0.0184. The amount of MPTMS precursor species was fixed, so that approximately 10% of total silicon atoms were functionalized with propyl-sulfonic acid groups.

Arene-sulfonic-acid functionalized mesostructured silica and organosilica were synthesized similarly to that described for the propyl-sulfonic-acid functionalized mesoporous solids above [13]. In this case, following the prehydrolysis step of the alkoxysilane precursor species (TEOS or TEOS + BTSE), 2-(4-chloro-sulfonylphenyl)-ethyl-trimethoxysilane (CSPTMS, Gelest) was added. Afterwards, the synthesis proceeded as described above. Molar composition of the mixtures, relative to 4 g of triblock copolymer, were: (0.0369 - *x*) TEOS: (*x*/2) BTSE: (0.0041) CSPTMS: 0.24 HCl: ≈ 6.67 H_2O, with *x* being 0 or 0.0184. Similarly, the amount of CSPTMS precursor species was fixed, so that approximately 10% of total silicon atoms were functionalized with arene-sulfonic-acid groups.

2.2 Catalyst characterization

X-ray powder diffraction (XRD) patterns were acquired on a PHILIPS X`PERT diffractometer using Cu K_α radiation. The data were recorded from 0.6 to 5º (2θ) with a resolution of 0.02º. Nitrogen adsorption and desorption isotherms at 77 K were measured using a Micromeritics TRISTAR 3000 system. The data were analysed using the BJH model on the adsorption branch of the isotherm, and the pore volume (*V*p) was taken at point where P/Po= 0.975 single point. Transmission electron micrographs (TEM) were obtained using a JEOL 2000 electron microscope operating at 200 kV.

Content and thermal stability of the organic and sulfonic-acid species within the mesoporous and organosilica materials were evaluated by elemental analysis (HCN) in a Vario EL III apparatus, and also indirectly by means of thermogravimetry analysis

(TGA) (SDT 2960 Simultaneous DSC-TGA, from TA Instruments). Samples were heated in a Mettler TGA/sDTA-851e ThermoGravimetric Analyzer from 25 ° to 800 °C at a rate of 10 °C/min under constant nitrogen gas flow of 50 mL/min. The concentrations of surface sulfonic acid groups were determined as cation-exchange capacities by titration with 0.01 M NaOH [11]. Table 1 summarizes data related to incorporation of the organic species and the resulting acidic properties.

Temperature Programmed Desorption (TPD) experiments were carried out in a Micromeritics AutoChem 2910 equipment provided with thermal conductivity detector (TCD) using helium as carrier gas. Prior to the TPD experiment, the sample was outgassed by thermal treatment in He flow. After cooling, the material was contacted with gas-phase water until saturation by successive injections of pulses, in amounts ranging from 0.1 to 2 μL. Reversibly adsorbed water was then removed in He flow for 2 h at 40 ºC. TPD tests were carried out by heating the sample from 40 to 400 ºC at 15 ºC min^{-1} with constant He flow, keeping the final temperature for an additional period of 15 min. The effluent was continuously screened for water detection by means of a TCD detector. From TPD curves, the amount of water retained and desorbed (W_{H2O}) and the temperature corresponding to the maximum of the desorption peak (T_{H2O}) are obtained.

Solid-state two-dimensional (2D) $^{13}C\{^{1}H\}$ and $^{29}Si\{^{1}H\}$ HETeronuclear chemical shift CORrelation (HETCOR) NMR experiments were performed on a Bruker AVANCE-500 NMR spectrometer operating at 500.13 MHz, 125.76 MHz, and 99.35 MHz for ^{1}H, ^{29}Si, and ^{13}C, respectively. Experiments were conducted at room temperature under magic-angle spinning (MAS) conditions at 10 kHz by using a Bruker $^{1}H/X$ double-resonance MAS probehead with 4.0-mm zirconia rotors. The HETCOR technique allows different dipole-dipole-coupled moieties to be differentiated and identified by spreading their chemical shifts into a 2D frequency map. The HETCOR

experiment is similar to standard cross-polarization magic-angle spinning (CP-MAS) NMR,[40] with the key exception that the ^{1}H magnetization is allowed to evolve for an incremented evolution time period t_1 prior to magnetization transfer to heteronuclei, such as ^{13}C or ^{29}Si, whose responses are measured directly during the detection period t_2 [41]. Double Fourier transformation converts the time domain signal $S(t_1,t_2)$ into the frequency domain $F(\omega_1,\omega_2)$, which is typically presented as a 2D contour plot spectrum. For the $^{13}C\{^{1}H\}$ HETCOR experiments, a 4.2 μs 90° pulse, followed by a 3 ms contact time, were used for cross-polarization. 864 acquisitions with a 2 s recycle delay were collected for 96 t_1 increments. For the $^{29}Si\{^{1}H\}$ HETCOR experiments, a 6.8 μs 90° pulse, followed by a 2 ms contact time, were used for cross-polarization. 768 acquisitions with a 2 s recycle delay were collected for 128 t_1 increments. The ^{1}H and ^{29}Si chemical shifts were referenced to tetrakis(trimethylsilyl)silane $[(CH_3)_3Si]_4Si$, and the ^{13}C chemical shift was referenced to adamantane ($C_{10}H_{16}$). All of the 2D HETCOR spectra are presented with contour levels shown to 20% of full intensity.

2.3 Catalytic reaction tests

Etherification experiments were carried out in liquid phase at 50 ºC in a stirred Teflon®-lined stainless-steel autoclave under autogenous pressure (with an initial nitrogen pressure of 4 bar to ensure that a liquid phase is maintained). Reaction temperature was controlled using a thermocouple immersed into the reaction mixture. Samples were periodically withdrawn at time intervals ranging from 0 to 2 h. Typically, weight composition of the reaction mixture was: 30 g of 1-hexanol, 3 g of vanillyl alcohol and constant catalyst loading of 0.03 g (0.1 wt%). Reaction samples were analyzed by GC (Varian 3900 chromatograph) using a CP-SIL 8 CB column (30m x 0.25 mm, film thickness = 0.25) and a flame ionization detector. Benzyl ether was the

only detected reaction product, and a control blank reaction gave no conversion of vanillyl alcohol in absence of acid catalyst. Catalytic results are shown either in terms of absolute conversion of vanillyl alcohol or in terms of initial rate values (mmol of reacted alcohol per g of catalyst and minute), calculated at the beginning of the reaction (15 min). To allow the comparison of the catalytic activity between different types of sulfonic acid groups (in different surface micro-environments), a specific initial rate per acid site has also been utilized (mmol of reacted alcohol per minute and mmol of acid site after 15 min of reaction).

3. Results and discussion

3.1. Catalyst structures, compositions and stabilities

Nitrogen adsorption isotherms measured for the sulfonic-acid functionalized materials were of Type IV according to IUPAC classification (Figure 1). For materials synthesized without BTSE, the isotherms displayed a pronounced hysteresis loop at relative pressures in the range 0.6-0.8, consistent with data previously reported [11, 13]. The increase in adsorption in the mesoporous range is less defined in the sulfonic acid-modified PMOs. Likewise, regardless of the type of sulfonic acid moiety, a gradual increase in the final nitrogen adsorbed volume at $P/Po>0.8$ is observed in the hybrid PMO materials. This unexpected increase in the adsorbed volume at high relative pressures might be attributed either to macropores or to interparticulate porosity, which takes place when the particle diameters are very small and closely packed. Thus, this effect might be related to a morphology change in the particles when introducing BTSE in the synthesis of the sulfonic-acid modified mesostructured materials (see TEM images in Supplementary Information; Figure SI.1).

Powder X-ray diffraction analyses of propyl- and arene-sulfonic acid functionalized samples give diffractograms that are typical signals for hexagonally-ordered mesopores [42] (Figure 1). Samples without ethylsiloxane functionalities in the composition of their pore walls, present the typical small-angle X-ray scattering (SAXS) reflections associated with *p6mm* symmetry. The organically-modified samples (PMOs) have in common a single prominent SAXS reflection centered at 2θ below 1º, assigned to the crystallographic direction [100]. The signals [110] and [200], indicative of long-range hexagonal ordering, are less pronounced than in the silica materials. This kind of diffraction pattern has been previously associated with "worm-hole" structures [43-44], and similar to those described in literature for related organically modified solids [45-46].

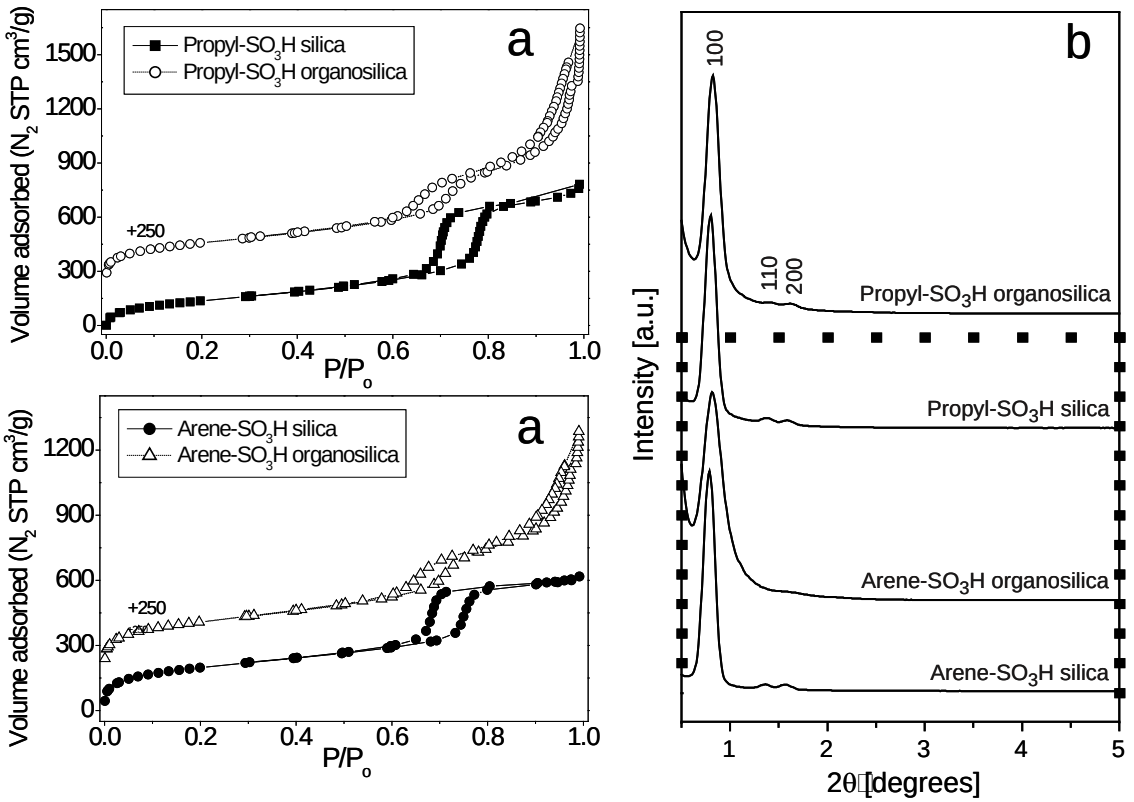

Figure 1. (a) Nitrogen adsorption isotherms at 77 K and (b) Small-angle X-ray scattering patterns for sulfonic-acid modified mesostructured silicas. See Table SI.1 in supplementary information, which summarizes the textural properties of these materials.

Elemental analyses and acid titration studies establish the incorporation of organic species within the silica framework and the accessibilities of the sulfonic-acid sites at the mesopore surfaces. Comparison of the sulfur concentrations determined by elemental analysis and the proton concentrations determined by cationic-exchange of the acid sites by sodium ions (Table 1) reveal that > 95% of the acid catalyst sites are accessible. In addition, the presence of ethylsiloxane moieties in the silica framework does not appear to affect the incorporation of sulfonic-acid species into the material. Further analysis of the incorporated sulfonic-acid and organic functionalities by single-pulse ^{29}Si MAS NMR (Table 1) establishes that the propyl- and arene-sulfonic-acid species are inserted into the silica framework to comparable extents. For example, single-pulse ^{29}Si MAS NMR analyses provide quantitative information on the relative populations of ^{29}Si sites resolved for different silica and organosilica moieties associated with the mesopore frameworks. Linewidths of approximately 9 ppm are observed for ^{29}Si signals associated with these materials, consistent with a large distribution of local ^{29}Si sites in the disordered silica frameworks. Nevertheless, single-pulse ^{29}Si MAS NMR spectra reveal resolved signals from ^{29}Si sites with different extents of condensation and numbers of organic ligands. Quantitative intensities are observed and attributed to the following silica and organosilica ^{29}Si species: Q^n = $Si(OSi)_n(OH)_{4-n}$, where n = 2-4 (Q^2 at ca. -90 ppm, Q^3 at ca. -100 ppm, and Q^4 at ca. -110 ppm), and T^m = $RSi(OSi)_m(OH)_{3-m}$, where m = 2-3 (T^3 at ca. -65 ppm and T^2 at ca. -57 ppm). Both the propyl- and arene-sulfonic-acid functionalized materials provide ratios of T^m signals that are consistent with bulk elemental analyses (Table 1). Furthermore, the ^{29}Si signal intensities assigned to T^m silicon atoms account not only for ethoxysilane functionalities, but also for the sulfonated species, propyl-SO_3H and arene-SO_3H. Combining the number of T^m sites from ^{29}Si MAS NMR (i.e., the number of Si–

R moieties) with carbon elemental analyses (Table 1), the differences in carbon concentrations in the propyl- and arene-sulfonic acid functionalized materials are consistent with the different molecular weights of the functional groups and not differences in their respective loadings.

Table 1. Sulfonic acid and organic contents of the sulfonic-acid-functionalized mesoporous silica and organosilica catalysts.

Catalyst	Elemental Analysis [a]		^{29}Si MAS NMR	Titration
	Sulfur content (mmol S/g SiO_2)	Carbon content (mmol C/g SiO_2)	T^m sites (mole %) [b]	Acid capacity (mmol H^+/g SiO_2)
Propyl-SO_3H silica	1.52 (±0.12)	6.15 (±0.35)	11	1.58
Propyl-SO_3H organosilica	1.53 (±0.18)	15.44 (±0.65)	57	1.45
Arene-SO_3H silica	1.66 (±0.08)	16.10 (±0.53)	12	1.71
Arene-SO_3H organosilica	1.79 (±0.21)	25.20 (±1.08)	56	1.83

[a] Mean values and experimental error obtained from three analysis replications.
[b] Molar percentage of T^m sites obtained from ^{29}Si MAS NMR spectra as follows = [Integrated Area of T^m signals/(Area T^m signals+ Area Q^n signals)]·100.

High thermal stabilities of incorporated sulfonic-acid and organic framework species are important in acid-functionalized mesoporous silica and organosilica catalysts. The main advantage of using the co-condensation method for inclusion of functional species in mesoporous silicas is the introduction of thermally-stable covalent Si–C anchoring bonds with high incorporation yields, in contrast to low incorporation typically obtained by post-synthetic grafting methods. Thermogravimetric analyses (see Supplementary Information, Figure SI.2) of the acid-functionalized mesoporous catalyst materials typically show weight loss profiles that can be divided into three regions: (1) from room temperature to 150 ºC attributed to water desorption, (2) between 150 ºC to 350 ºC, attributed to remaining surfactant molecules and surface-adsorbed ethoxy groups from the ethanol-extraction to remove the surfactant species, and (3) above 350 °C, from the thermal decomposition of sulfonic-acid groups and ethylsiloxane moieties within the

silica framework. Higher mass losses are observed in region 3 for the organosilica materials compared to the silica materials (19.5 % vs. 13.2 % for the propyl-sulfonic acid materials and 25.5 % vs. 18.4 % for the arene-sulfonic acid materials), in spite of having a constant sulfonic-acid functionality loading. The increased mass loss above 350 °C is quantitatively consistent with simultaneous decomposition of the ethylsiloxane and sulfonic-acid moieties in the organosilica materials. Progressive decomposition of the ethylsiloxane moieties over a wide temperature range is evidence of a distribution of local environments around the framework ethylsiloxane functionalities. Notably, the mass loss assigned to water desorption is lower by ~ 2 % in the organosilicas compared to the silica materials. The difference, although small, is indicative of the more hydrophobic nature in the ethylsiloxane-modified organosilica materials, even in the presence of highly hydrophilic sulfonic-acid species.

3.2 Catalyst performance

Propyl- and arene-sulfonic acid modified mesostructured SBA-15 silicas have previously been demonstrated as active catalysts in the etherification of benzyl alcohols, and for which the hydrophobicity of the local environment surrounding the acid sites plays a key role in the catalytic performance [47]. The sulfonic-acid catalyst sites are readily poisoned by water as reaction by-product. Balancing the hydrophobic-hydrophilic surface properties of the catalyst allows one to modulate the reaction conversion rates. Here, the etherification of vanillyl alcohol (4-hydroxy-3-methoxybenzylalcohol) with 1-hexanol to yield 4-hydroxy-3-methoxybenzyl-1-hexyl ether (Scheme 1) has been chosen as a technologically-relevant, acid-catalyzed reaction to examine the effects of increased hydrophobicity of the mesoporous organosilica support material on the acid-catalyst performance.

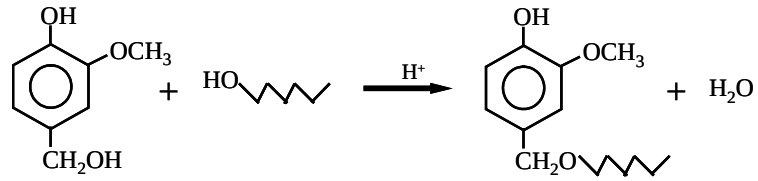

Scheme 1. Production of 4-hydroxy-3-methoxybenzyl-1-hexyl ether via the etherification of vanillyl alcohol and 1-hexanol.

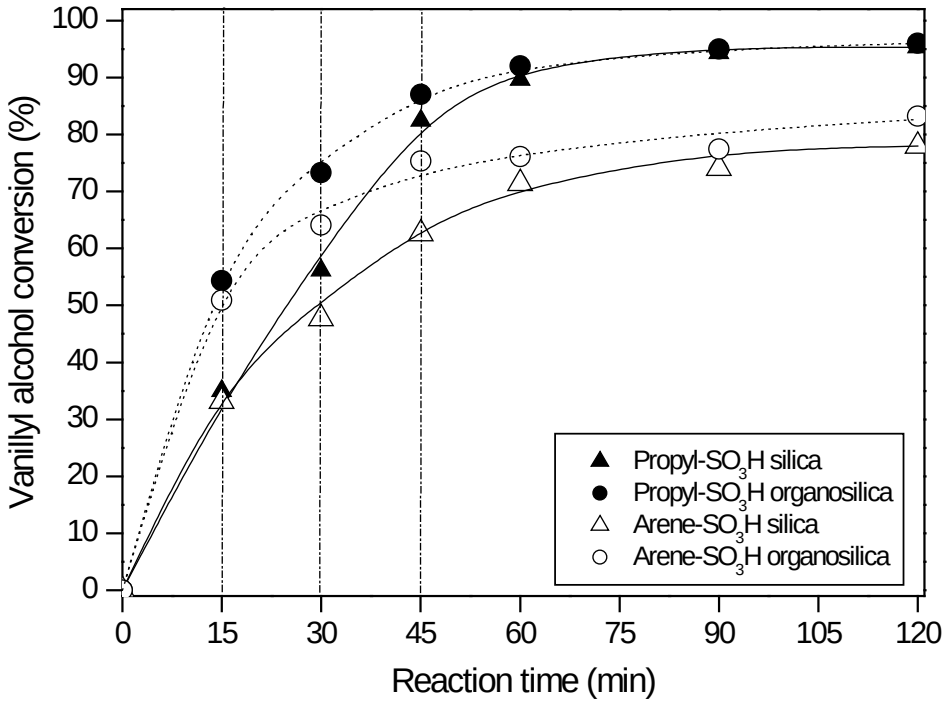

Figure 2. Etherification of vanillyl alcohol with 1-hexanol over propyl- and arene-sulfonic-acid modified mesoporous silica and organosilica catalysts. Reaction conditions: batch reactor at 50 ºC and 4 bar; 30 g 1-hexanol, 3 g vanillyl alcohol, 0.03 g catalyst (0.1 wt %).

Comparisons of vanillyl alcohol conversion in batch reactions over propyl- and arene-sulfonic-acid mesoporous silica and organosilica catalysts establish the beneficial performance effects of incorporating hydrophobic ethylsiloxane moieties in the mesoporous silica support. As shown in Figure 2, both propyl- and arene-sulfonic-acid species on mesoporous silica display high conversion rates, reaching conversions of over 77% (arene-SO_3H) and over 95% (propyl-SO_3H) after only 2 h of reaction.

Despite their lower acid strength, the propyl-sulfonic acid sites exhibit higher etherification activity than the arene-sulfonic-acid groups. This is attributed to lower hydrophilicity of the alkyl chain, compared to the aromatic ring, which yields local environments near the sulfonic-acid active sites that are less sensitive to the poisoning effect of co-adsorbed water molecules. This is further supported by the activities measured for the propyl-SO_3H and arene-SO_3H groups anchored on more hydrophobic mesoporous organosilica supports.

For both the propyl- and arene-sulfonic acid functionalized mesoporous organosilicas, clear improvements in their respective etherification activities are observed compared to otherwise identical mesoporous silica-supported SO_3H catalysts. This improvement is especially apparent at initial reaction times, where deactivation effects are minimal and the conditions are far away from chemical equilibrium. The acid-functionalized mesoporous organosilica catalysts show higher initial conversions of vanillyl alcohol after 15 min reaction time, compared to the corresponding acid-functionalized mesoporous silica catalysts (Table 2). Furthermore, assuming linear behavior during the first 15 min, initial reaction rates are also about 1.5 higher when using the organosilica catalysts. Normalizing the initial reaction rates per acid site (r_o'), the enhancement of catalytic activity in the organosilicas compared to the silica materials is even higher (1.8 times higher in the case of propyl-SO_3H organosilica). Incorporation of hydrophobic ethylsiloxane moieties into the silica support framework has a beneficial effect on the catalyst performance, presumably due to reduced water poisoning of the acid active sites.

Table 2. Catalytic activity of propyl- and arene-sulfonic acid modified mesoporous silica and organosilica catalysts in the etherification of vanillyl alcohol with 1-hexanol.

Catalyst	$X_{vanillyl}$ [a]	r_o [b]	r_o' [c]
Propyl-SO_3H silica	35	14.4	11.7
Propyl-SO_3H organosilica	54	22.2	21.2
Arene-SO_3H silica	33	13.6	11.1
Arene-SO_3H organosilica	51	21.0	16.9

[a] Conversion of vanillyl alcohol at 15 min.
[b] Initial reaction rate values [(mmol)·(g_{cat}^{-1})·(min^{-1})] calculated from mmols of reacted vanillyl alcohol within the first 15 min of reaction per gram of catalyst.
[c] Initial specific reaction rate values per acid site [(mmol)·(mmol acid-$center^{-1}$)·(min^{-1})] calculated from mmols of reacted vanillyl alcohol within the first 15 min of reaction and referred to mmol of acid sites per gram of each catalyst.

3.3 Water retention capacities

The comparison of the bulk hydrophilicities of acid-functionalized mesoporous silica and organosilica catalysts confirms that incorporation of ethylsiloxane moieties within the silica frameworks reduces the water retention capacities of the material. Temperature-programmed-desorption (TPD) were performed to study the interaction of adsorbed water with the acid-functionalized surfaces of the mesoporous silica and organosilica materials. The TPD curves for water over sulfonic-acid modified mesoporous silica and organosilica samples show two desorption peaks, the first one (100-200 ºC) corresponding to the desorption of water interacting strongly with acid sites. Desorption signal over 200 ºC would be attributed to thermal decomposition of SO_3H and Si-CH_2-CH_2-Si moieties, and to dehydration of surface Si-OH groups. This assumption is valid since decomposition of acid and ethylene moieties occurs at higher temperature ranges (observed in TGA data [14]). Furthermore, Shimizu et al. [48] also employed this approximation for TPD results over sulfonic-acid modified silica samples. It should be noted that the adsorbed-desorbed amounts of water shown in Table 3 correspond to dynamic experiments in continuous helium flow with a previous physi-desorption step at 40 ºC to remove weakly retained water. Accordingly, the

amounts shown account only for water that is more strongly bounded to the functionalized surfaces and are significantly smaller than the adsorption capacity corresponding to the total pore filling of the mesopores. Thus, the relative amounts of desorbed water in TPD experiments, shown in Table 3, can be used to compare the hydrophilicities of the samples.

Table 3. Temperature-Programmed-Desorption (TPD) of water in propyl- and arene-sulfonic-acid modified mesoporous silica and organosilica catalysts.

Mesoporous catalysts	T_{H2O} [a]	W_{H2O} [b]		
	(°C)	(mg/g)	(mmol/g)	(mmol H_2O/mmol H^+)
Silica	83	0.74	0.04	-
Propyl-SO_3H silica	119	13.81	0.77	0.62
Propyl-SO_3H organosilica	117	6.77	0.38	0.36
Arene-SO_3H silica	139	14.55	0.81	0.65
Arene-SO_3H organosilica	137	7.83	0.49	0.40

[a] Temperature corresponding to the maximum of the water desorption peak
[b] Water amount retained and desorbed by the solid in the temperature range of 50-200ºC

The sulfonic-acid modified mesoporous organosilicas are more hydrophobic than the corresponding sulfonic-acid modified mesoporopus silicas, although much less compared to mesoporous silica. As shown in Table 3, the sulfonic-acid organosilicas adsorb about half the amount of water (expressed as $mg \cdot g^{-1}$) than the sulfonic-acid silicas, and approximately 10 times that corresponding to pure silica. That is, the water-retention capacity is clearly increased by incorporating acid functional species, but reduced when incorporating alkyl moieties within the framework of the mesostructure. Additionally, the temperature corresponding to the peak of maximum desorption remains practically constant when considering catalyst supports functionalized by the same acid moiety (about 117-119 ºC for propyl-sulfonic-acid materials, and 137-139 ºC for arene-sulfonic-acid materials), which suggests that the interactions between the -SO_3H groups and water molecules does not depend strongly on the surface

hydrophobicity. Comparing the effect of neighboring molecular groups adjacent to the $^{-}SO_3H$ sites, arene-sulfonic-acid materials provide slightly higher water loadings and retain water to much higher retention temperatures relative to the propyl-sulfonic acid materials, in agreement with enhanced acid strengths and resulting hydrophilicities.

A consequence of this is that the acid centers may be subjected to H_2O-poisoning in reactions involving non-polar organic molecules. Hence, the higher catalytic performance displayed by the SO_3H-modified PMO samples might be attributed to weaker interactions between the sulfonic-acid groups in these catalysts and water molecules generated during reaction (Scheme 1). This is expected to lead to better accessibilities of alcohol reactant molecules to the sulfonic-acid active sites. Since the $^{-}SO_3H$ moieties are highly hydrophilic, the hydrophobicity of the nearby acid site environments exert substantial influence on their activities in water-sensitive organic reactions. Macroscopically, the water-retention properties of these materials, as determined by TGA and H_2O-TPD measurements (Table 3), and the catalytic results obtained in the etherification of vanillyl alcohol with 1-hexanol (Figure 2) are consistent with this hypothesis. However, insights and understanding of the molecular origins of these macroscopic adsorption and reaction behaviours remain unknown.

3.3 Local site compositions and structures

Powerful two-dimensional (2D) nuclear magnetic resonance (NMR) spectroscopy techniques are especially sensitive to local compositions, structures, and dynamics of framework, functional, and adsorbed species in the mesoporous organosilica catalysts. In particular, 2D $^{13}C\{^{1}H\}$ and $^{29}Si\{^{1}H\}$ HETCOR measurements provide significantly enhanced spectral resolution and clear identification of otherwise overlapping 1D ^{1}H signals associated with the various dipole-dipole-coupled molecular moieties in acid-

functionalized mesoporous materials. For the arene- or propyl-SO_3H-modified catalysts under consideration here, these include grafted sulfonic acid species, framework ethylsiloxane moieties, and weakly surface-adsorbed ethoxy groups from either ethanol washing or non-condensed ethoxysilanes (Figs. 3a, 4a, 5a, 6a). In a 2D HETCOR spectrum, correlated ^{1}H and ^{13}C or ^{29}Si signal intensities can be observed for directly bonded or spatially proximate (ca. 1 nm) species. By adjusting the $^{1}H \rightarrow ^{13}C$ or $^{1}H \rightarrow ^{29}Si$ cross-polarization contact times, it is furthermore possible to distinguish between strongly and weakly interacting species. By this method, unambiguous information is obtained on molecular-level structures and local compositions in acid-functionalized mesoporous catalysts that account for differences in their macroscopic catalytic properties.

Arene-SO_3H-functionalized mesoporous silica and organosilica catalysts

Specifically, 2D HETCOR spectra allow different grafted, surface-adsorbed, and framework moieties to be identified and their mutual proximities established. Moreover, differences in the extents to which arene- and propyl-sulfonic acid-functionalized mesoporous silica or mesoporous organosilica materials adsorb water can be understood at a molecular-level and correlated with their efficacies for catalyzing heterogeneous etherification reactions, such as the etherification of vanillyl alcohol with 1-hexanol. For example, Figure 3 shows 2D $^{13}C\{^{1}H\}$ HETCOR spectra obtained from arene-SO_3H acid-functionalized mesoporous silica (Fig. 3b) and mesoporous organosilica, (Fig. 3c) with the various proton moieties of the arene-sulfonic acid groups, surface-adsorbed ethoxy groups, framework ethylsiloxane groups, and adsorbed water all yielding well resolved signals. The 2D $^{13}C\{^{1}H\}$ HETCOR spectrum in Figure 3b shows strong correlated signal intensities at 1.2 ppm in the ^{1}H dimension and at 16

ppm and 28 ppm in the ^{13}C dimension, which are associated with the alkyl $–CH_2–$ groups (labeled ‘1’ and ‘2’ in Fig. 3a) of the arene-SO_3H species and the $–CH_3$ groups (labeled ‘5’ in Fig. 3a) of surface ethoxy species, respectively. The $–OCH_2–$ (4) groups of the surface ethoxy species give rise to 2D signal intensity at 3.8 ppm in the ^1H dimension and 58 ppm in the ^{13}C dimension. The aromatic protons of the arene-SO_3H species yield correlated 2D signal intensities at 7.6-8.0 ppm in the ^1H dimension and between 124-146 ppm in the aromatic region of the ^{13}C dimension. In addition to the signal intensities arising from directly bonded $^1H–^{13}C$ pairs, two clearly resolved signals in the 2D $^{13}C\{^1H\}$ HETCOR spectrum in Figure 3b at 6.4 ppm in the ^1H dimension and 124 ppm and 126 ppm in the ^{13}C dimension (dotted red lines) are attributed to adsorbed water molecules that are in close spatial proximity to the aromatic carbon atoms and $–SO_3H$ groups of the arene-sulfonic acid species.

By comparison, the 2D $^{13}C\{^1H\}$ HETCOR spectrum for the arene-sulfonic acid-functionalized organosilica catalyst (Figure 3c) shows the same correlations as for the wholly siliceous support with two notable exceptions. First, the additional correlated 2D signal intensity at 1.2 ppm in the ^1H dimension and 6 ppm in the ^{13}C dimension arises, due to the presence of $–CH_2–$ groups (‘3’ in Fig. 3a) associated with the ethylsiloxane species incorporated into the organosilica framework. Furthermore, while the single-pulse ^1H NMR spectrum shown along the ^1H dimension of the 2D contour plot contains an intense signal at 6.9 ppm corresponding to the adsorbed water, there is no 2D signal correlated to any of the ^{13}C species, including the aromatic carbon atoms adjacent to the $–SO_3H$ acid sites of the arene-sulfonic acid species. This is an important difference from the arene-sulfonic acid functionalized mesoporous silica catalyst. It establishes that upon incorporation of ethylsiloxane species into the mesoporous silica framework,

adsorbed water no longer resides in the local environments near (ca. 1 nm) the $-SO_3H$ catalytic acid sites.

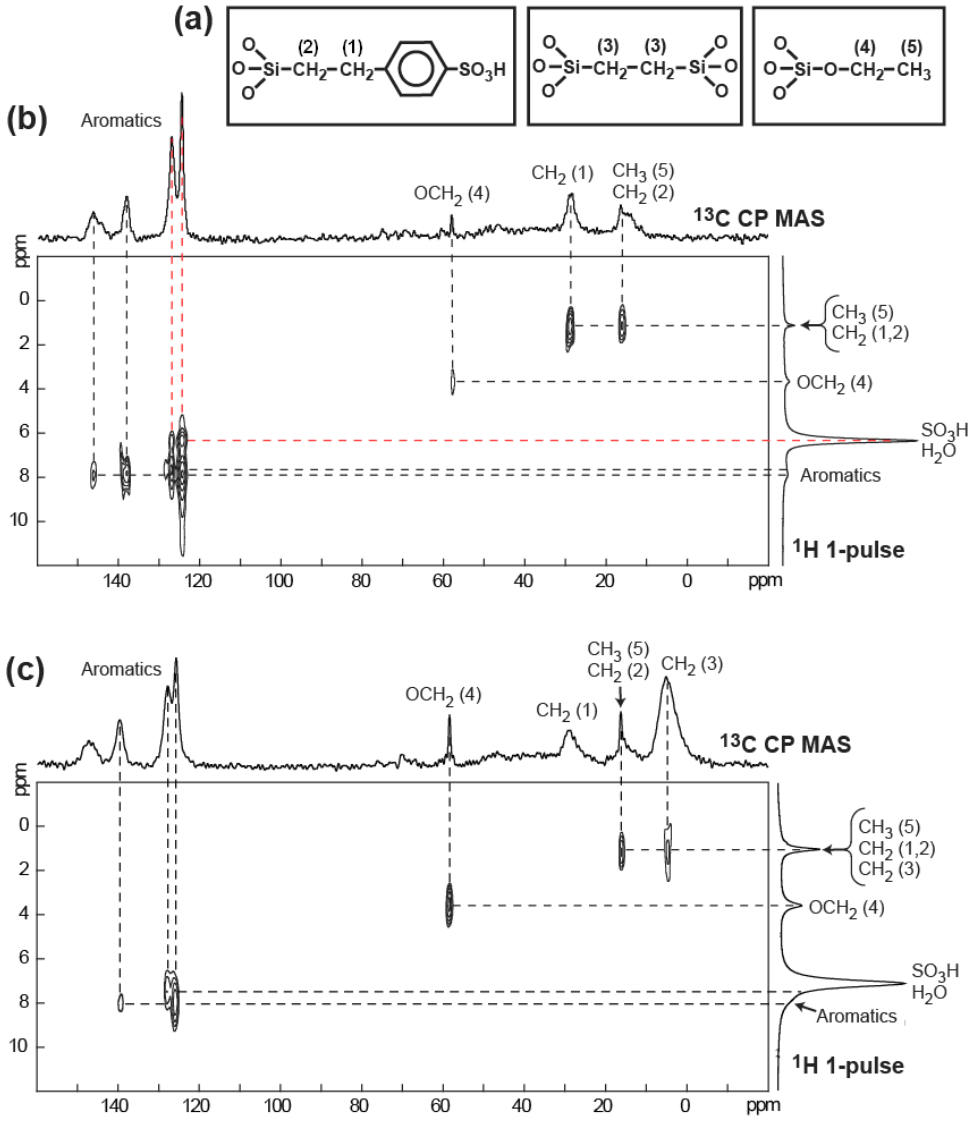

Figure 3. (a) Schematic representations of the organic moieties present and identified in room-temperature 2D $^{13}C\{^1H\}$ HETCOR spectra of (b) mesoporous silica and (c) mesoporous ethylsiloxane functionalized with arene-SO_3H moieties. Separate ^{13}C CP-MAS and ^1H MAS spectra are plotted along their corresponding axes. The 2D $^{13}C\{^1H\}$ HETCOR spectra show strongly correlated ^{13}C and ^1H signals that permit their unambiguous assignments to grafted arene-sulfonic acid moieties, surface ethoxy groups, framework ethylsiloxane moieties, and adsorbed water. Note the strong 2D intensity correlation (dotted red lines) between protons of adsorbed water and the aromatic ^{13}C nuclei in Figure 3(b) and its absence in Figure 3(c), which manifests the different hydrophilicities/hydrophobicities near the acid sites of the silica and organosilica supports.

The 2D $^{29}Si\{^{1}H\}$ HETCOR spectra acquired for the same arene-sulfonic acid-functionalized silica and organosilica catalysts confirm the covalent grafting of the acid moieties and corroborate the increased hydrophobicity of the mesoporous organosilica support. As shown in Figure 4 for both samples, 2D $^{29}Si\{^{1}H\}$ intensity correlations are clearly resolved between the alkyl protons of the arene-SO_3H species and the protons of adsorbed water molecules with the various ^{29}Si sites in the materials. For example, in Figure 4b, the $^{29}Si\{^{1}H\}$ HETCOR spectrum acquired for the arene-sulfonic acid functionalized silica (without ethylsiloxane incorporated) shows 2D signal intensity at 1.2 ppm in the ^{1}H dimension and -65 ppm in the ^{29}Si dimension. Such correlated intensity arises from dipole-dipole couplings between the $–CH_2–$ (1,2) protons of the arene-sulfonic acid moieties and cross-linked silica T^3 ^{29}Si sites associated with the silica framework (T^n refers to four-coordinate silica units with n (an integer≤3) silicon next-nearest neighbors, one covalent Si–C bond associated with an organic moiety, and (3-n) uncondensed Si–O bonds, e.g, hydroxyl species). In addition, strong 2D signal intensity is observed at 6.4 ppm in the ^{1}H dimension and -102 ppm in the ^{29}Si dimension, reflecting strong interactions between protons of adsorbed water molecules and partially polymerized Q^3 ^{29}Si sites. (Q^n refers to four-coordinate silica units with n (an integer≤4) silicon next-nearest neighbors and (4-n) uncondensed Si–O bonds, e.g, hydroxyl species). The T^3 ^{29}Si signal at -65 ppm in Figure 4b is also correlated with that of the ^{1}H nuclei of the adsorbed water molecules in the wholly siliceous silica support (6.4 ppm).

Similarly, for the arene-sulfonic acid functionalized organosilica, 2D $^{29}Si\{^{1}H\}$ HETCOR results confirm acid-group grafting and increased hydrophobicity of the mesoporous support. The 2D $^{29}Si\{^{1}H\}$ HETCOR spectrum in Figure 4c shows correlated signal intensity at 6.8 ppm in the ^{1}H dimension and -100 ppm and -110 ppm

in the ^{29}Si dimension (dotted red lines), corresponding to interactions between adsorbed water protons and both the Q^3 and spatially proximate, and presumably surface, Q^4 ^{29}Si sites in the framework. In addition, correlated intensity at 1.2 ppm in the ^{1}H dimension and -65 ppm in the ^{29}Si dimension is also observed, corresponding to interactions between the –CH_2– (1,2) protons of the arene-sulfonic acid moieties and the T^3 ^{29}Si framework sites; a weak intensity correlation is also observed at -55 ppm corresponding to incompletely cross-linked T^2 ^{29}Si sites. As expected for the organosilica support, higher populations of T^2 and T^3 ^{29}Si sites are present, relative to the Q^3 and Q^4 species and compared to the mesosporous silica catalyst, as established by the different integrated signal intensities in the one-pulse ^{29}Si MAS spectra in Figure 4b,c. The notable absence of any 2D signal intensity at 6.8 ppm in the ^{1}H dimension and -65 ppm in the ^{29}Si dimension establishes that adsorbed water molecules do not reside near (ca. 1 nm) a significant fraction of the arene-SO_3H moieties in the functionalized organosilica catalyst.

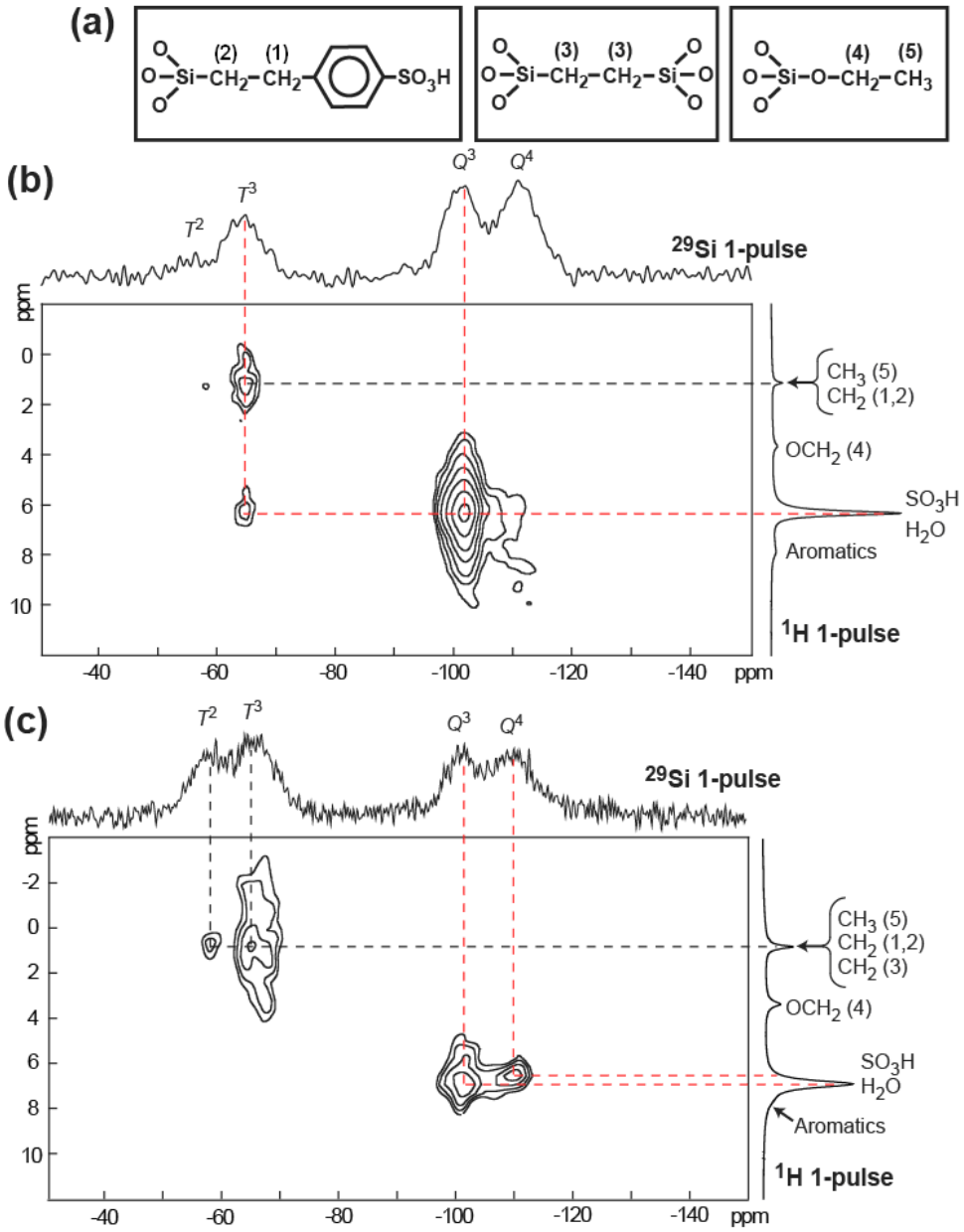

Figure 4. (a) Schematic representations of the various organic moieties present in arene-SO_3H-functionalized silica catalyst materials, with room-temperature 2D ^{29}Si{^{1}H} HETCOR spectra acquired for (b) mesoporous silica and (c) mesoporous organosilica (ethylsiloxane) supports. Separate one-pulse ^{29}Si and ^{1}H MAS spectra are plotted along their corresponding axes. All measurements were conducted on the same samples as used in Figure 3. The ^{29}Si{^{1}H} HETCOR spectra show strongly correlated signal intensities between ^{29}Si Q^3 and Q^4 framework sites and ^{1}H nuclei of the grafted sulfonic acid moieties and/or adsorbed water.

Propyl-SO_3H-functionalized mesoporous silica and organosilica catalysts

Similar corroborative results and conclusions are obtained from the propyl-sulfonic acid-functionalized silica and organosilica catalysts. The 2D ^{13}C{^{1}H} HETCOR spectra

shown in Figures 5b and 5c allow the various overlapping signals in the 1D single-pulse ^{1}H spectra from the propyl-sulfonic acid, surface ethoxy, and ethylsiloxane species (Fig. 5a) to be clearly resolved. For example in Figure 5b, 2D signal intensities from each of the different $–CH_2–$ (1,2,3) moieties of the propyl-sulfonic acid species at 1.1 ppm in the ^{1}H dimension are clearly resolved at 56 ppm, 18 ppm, and 4 ppm in the ^{13}C dimension. The $–OCH_2–$ moieties of the remaining surfactant yield weak 2D signal intensity at 3.8 ppm in the ^{1}H dimension and 71 ppm in the ^{13}C dimension. Notably, weak 2D correlated signal intensity is also observed at 6.5 ppm in the ^{1}H dimension and 56 ppm in the ^{13}C dimension, corresponding to interactions between the protons of adsorbed water molecules near the propyl–SO_3H groups and ^{13}C nuclei of the nearest $–CH_2–$ (1) moieties.

By comparison, the 2D $^{13}C\{^{1}H\}$ HETCOR spectrum in Figure 5c for the propyl-SO_3H-functionalized organosilica support shows signal intensities corresponding to the same correlations as in Figure 5b for the propyl-SO_3H-functionalized silica material, but with two important differences. An additional 2D signal is present in Figure 5c at 1.1 ppm in the ^{1}H dimension and 6 ppm in the ^{13}C dimension, corresponding to the $–CH_2–$ (4) groups of the incorporated framework ethylsiloxane species. Importantly, in addition, there is no 2D signal intensity in the spectrum near 7.0 ppm in the ^{1}H dimension and 56 ppm in the ^{13}C dimension, establishing that no detectable interactions are measured between adsorbed water and the ^{13}C nuclei adjacent to the propyl-sulfonic acid sites. This corroborates at a molecular level the greater hydrophobicity of the organosilica-supported propyl-SO_3H catalysts.

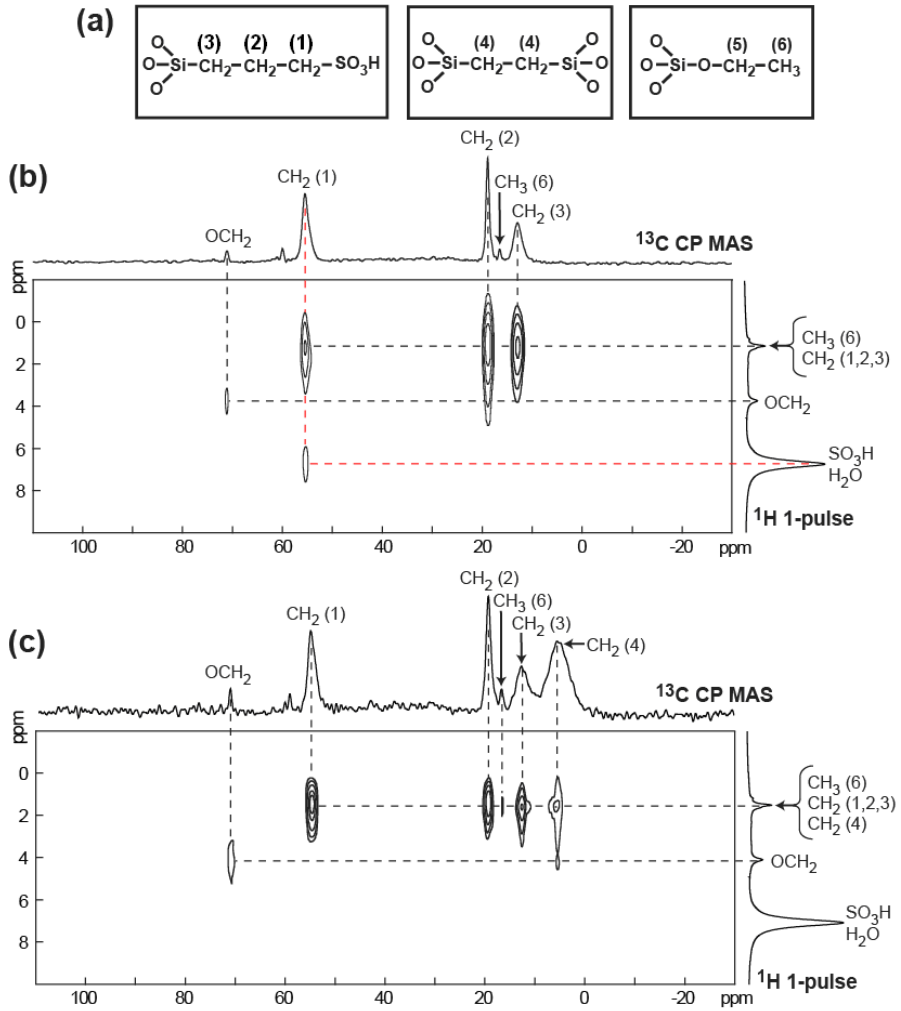

Figure 5. (a) Schematic representations of the organic moieties present and identified in room-temperature 2D $^{13}C\{^{1}H\}$ HETCOR MAS spectra of (b) mesoporous silica and (c) mesoporous organosilica functionalized with propyl-SO_3H acid moieties. Separate ^{13}C CP-MAS and ^{1}H MAS spectra are plotted along their corresponding axes. The 2D $^{13}C\{^{1}H\}$ HETCOR spectra show similarly strongly correlated ^{13}C and ^{1}H signals from grafted propyl-sulfonic acid moieties, surface and framework organic groups, and adsorbed water. The strong 2D intensity correlation (dotted red lines) observed in Figure 5 (b) between protons of adsorbed water and the propyl ^{13}C nuclei is absent in Figure 5 (c), manifesting the very different hydrophilic/hydrophobic environments near the acid sites of the silica and organosilica supports.

Likewise, comparing spectra in Figure 5 (propyl-SO_3H catalysts) with those in Figure 3 (arene-SO_3H catalysts), higher intensity in the correlation between water protons (signal in the spectra near 7.0 ppm in the ^{1}H dimension) and the corresponding ^{13}C nuclei next to the sulfonic acid sites (aromatic ^{13}C nuclei at 124-146 ppm for arene-SO_3H catalysts and alkyl ^{13}C nuclei at 54 ppm for propyl-SO_3H catalysts in the ^{13}C dimension) is clearly evidenced, especially for the silica materials (spectra denoted as

b). This confirms the macroscopic information above presented from catalytic and TPD data, where the environment in propyl-SO_3H sites is more hydrophobic than in arene-SO_3H moieties.

The 2D $^{29}Si\{^1H\}$ HETCOR spectra acquired for the same propyl-sulfonic acid-functionalized silica and organosilica catalysts confirm the covalent grafting of the acid moieties and corroborate the increased hydrophobicity of the mesoporous organosilica support. As shown in Figure 6 for both the silica and organosilica supports, 2D $^{29}Si\{^1H\}$ HETCOR spectra show correlated signal intensity between protons associated with the alkyl $–CH_2–$ (1,2,3) groups or adsorbed water and various ^{29}Si sites in the materials. For example, in Figure 6b, the 2D $^{29}Si\{^1H\}$ HETCOR spectrum acquired for the wholly siliceous mesoporous support shows strong correlated signal intensities at 6.5 ppm in the ^1H dimension and -100 and -110 ppm in the ^{29}Si dimension (dotted red lines) , corresponding to strong interactions between adsorbed water molecules and the Q^3 and Q^4 ^{29}Si sites, respectively, in the silica framework. In addition, the T^3 ^{29}Si sites share strongly correlated 2D signal intensity at -67 ppm with the alkyl protons of the propyl-sulfonic acid species at 1.1 ppm.

Similarly, for the propyl-sulfonic acid-functionalized organosilica, 2D $^{29}Si\{^1H\}$ HETCOR results confirm acid-group grafting and increased hydrophobicity of the mesoporous support. The 2D $^{29}Si\{^1H\}$ HETCOR spectrum in Figure 6c shows the same correlated signals associated with water-Q^3/Q^4 interactions (dotted red lines) as for the wholly siliceous mesoporous support, although with weaker intensities. This is consistent with the more hydrophobic character of the ethylsiloxane-incorporated organosilica support. In addition, a weak correlation is also observed between the $–CH_2–$ (1,2,3) protons (1.2 ppm) of the propyl-sulfonic acid moieties with the incompletely cross-linked T^2 ^{29}Si sites (-55 ppm). Finally, as in Figure 6b, there is no

2D signal intensity arising from interactions between the acid grafting sites (T^n ^{29}Si species) and adsorbed water protons. These results confirm the increased hydrophobicity of mesopore surfaces in the propyl-SO_3H-functionalized organosilica mesoporous catalyst.

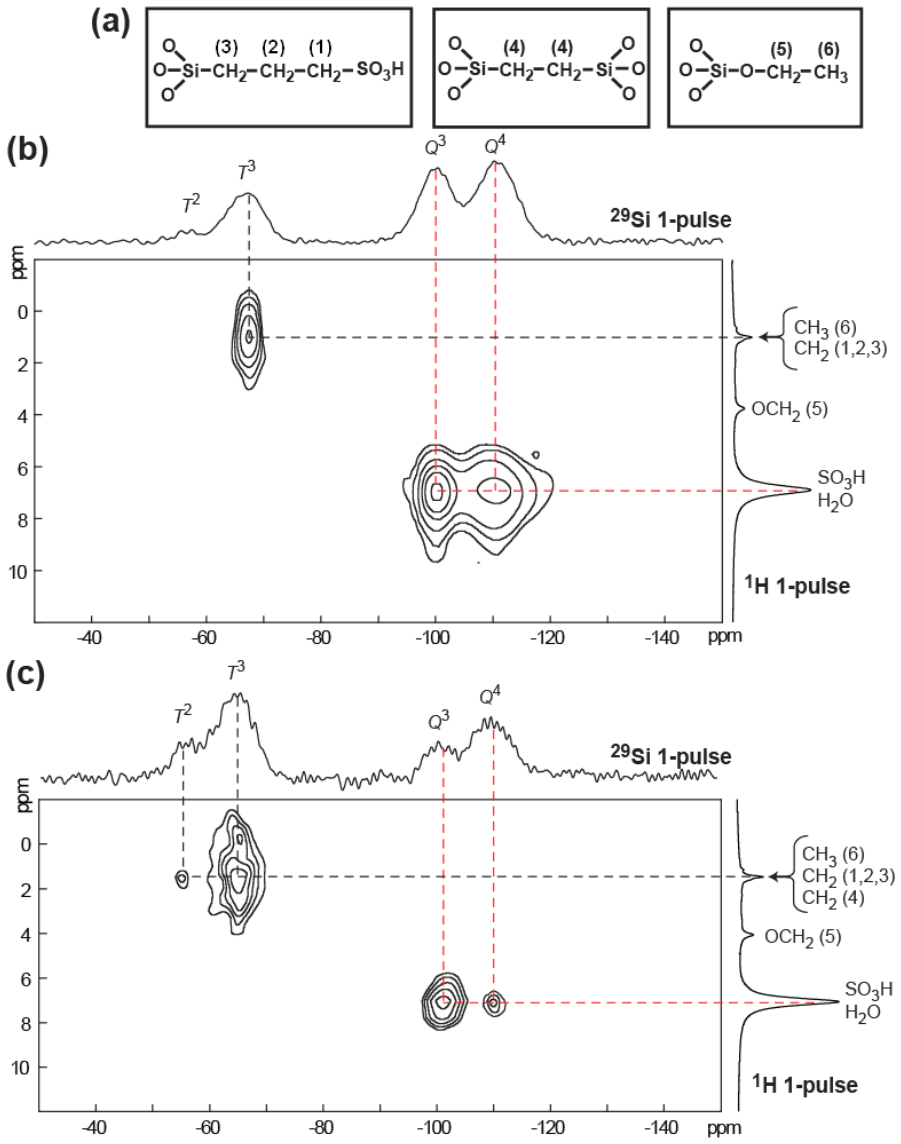

Figure 6. (a) Schematic representations of the various organic moieties present in propyl-SO_3H-functionalized silica catalyst materials, with room-temperature 2D ^{29}Si{^{1}H} HETCOR spectra for (b) mesoporous silica and (c) mesoporous organosilica (ethylsiloxane) supports. Separate one-pulse ^{29}Si and ^{1}H MAS spectra are plotted along their corresponding axes. All measurements were conducted on the same samples as used in Figure 5. The ^{29}Si{^{1}H} HETCOR spectra show strongly correlated signal intensities between ^{29}Si Q^3 and Q^4 framework sites and ^{1}H nuclei of the grafted SO_3H moieties and/or adsorbed water.

As discussed before for the $^{13}C\{^{1}H\}$ HETCOR spectra, comparing $^{29}Si\{^{1}H\}$ HETCOR spectra in Figure 4b (propyl-SO_3H silica) and Figure 6b (arene-SO_3H silica), a clear difference in the correlation between water protons (signal in the spectra near 7.0 ppm in the ^{1}H dimension) and the T^3 ^{29}Si species (at -67 ppm in the ^{29}Si dimension) is deduced. While in the case of arene-SO_3H silica such a correlation is evident, for the propyl-SO_3H no interaction can be observed. Again, this confirms that the environment in propyl-SO_3H sites is more hydrophobic than in arene-SO_3H moieties.

Conclusions

The incorporation of hydrophobic ethylsiloxane units within the frameworks of propyl- and arene-SO_3H-modified mesoporous silica materials have been shown to provide enhanced catalytic activities for the etherification of vanillyl alcohol and 1-hexanol. Water produced as a by-product of the reaction coadsorbs near the sulfonic acid centers, resulting in their partial deactivation due to competition with the alcohol reactant species. The 2D $^{13}C\{^{1}H\}$ and $^{29}Si\{^{1}H\}$ HETCOR NMR results establish unambiguously that the incorporation of ethylsiloxane moieties into the silica framework of mesoporous acid catalysts introduces important hydrophobicity locally around the sulfonic acid catalyst sites. In both the arene- and propyl-SO_3H-functionalized catalysts, the 2D $^{13}C\{^{1}H\}$ HETCOR spectra prove that the hydrophobic ethylsiloxane groups in the organosilica framework lead to reduced interactions of adsorbed water with the sulfonic acid catalyst sites. The 2D $^{29}Si\{^{1}H\}$ HETCOR results, furthermore, establish that interactions between adsorbed water molecules and ^{29}Si sites on the interior mesopore surfaces are also diminished upon the incorporation of ethylsiloxane groups in the silica framework. These results are in agreement with the

lower water-retention capacities, as determined by means of TPD and TGA, and higher etherification activities of SO_3H-functionalized mesoporous organosilicas, compared to wholly siliceous mesoporous supports. Despite their lower intrinsic acid strengths, propyl-SO_3H acid sites yield higher catalytic activities than arene-SO_3H groups; more hydrophobic local environments near the propyl-sulfonic acid sites result in reduced poisoning by adsorbed water. The relationships between the macroscopic catalytic behaviors and molecular surface properties of the materials are expected to be generally applicable to other water-sensitive reactions, where hydrophilic/hydrophobic interactions among reacting species and active/adsorption sites must be balanced.

Acknowledgements

Spanish co-authors thank the research project CICYT (CTQ2005-02375) for financial support. The UCSB co-authors' contributions were supported in part by the U.S. Department of Energy, Office of Basic Energy Sciences, Catalysis Sciences Grant No. DE-FG02-03ER15467 and by MURI program of the USARO under grant No. DAAD 19-03-1-0121. The 2D NMR measurements made use of the Central Facilities of the UCSB Materials Research Laboratory supported by the MRSEC Program of the NSF under award No. DMR 05-20415. B.F.C. thanks the Spanish Ministerio de Educación y Cultura for fellowship support during a recent sabbatical visit.

References

[1] T. Okuhara, Chem. Rev. 102 (2002) 3641.

[2] J. H. Clark, D. J. Macquarrie, Handbook of Green Chemistry and Technology, Blackwell, Oxford (2002).

[3] M. A. Harmer, W.E. Farneth, Q. Sun, Adv. Mater. 10 (1998) 1255.

[4] K. Wilson, J.H. Clark, Pure Appl. Chem. 72 (2000) 1313-1319.

[5] A. Vinu, K. Z. Hossain, K. Ariga, J. Nanosci. Nanotechnol. 5 (2005) 347.

[6] G. Oye, J. Sjoblom, M. Stocker, Adv. Colloid Interface Sci. 89-90 (2001) 439.

[7] A. Corma, Chem. Rev. 97 (1997) 2373.

[8] W. Van Rhijn, D. De Vos, W. Bossaert, J. Bullen, B. Wouters, P. Grobet, P. A. Jacobs, Stud. Surf. Sci. Catal. 117 (1998) 183.

[9] W. M. Van Rhijn, D.E. De Vos, B.F. Sels, W. D. Bossaert, P.A. Jacobs, Chem. Commun. (1998) 317.

[10] M.H. Lim, C. F. Blanford, A. Stein, Chem. Mater. 10 (1998) 467.

[11] D. Margolese, J.A. Melero, S.C. Christiansen, B. F. Chmelka, G. D. Stucky, Chem. Mater. 12 (2000) 2448.

[12] I. Díaz, F. Mohino, J. Pérez-Pariente, E. Sastre, Appl. Catal. A: Gen. 205 (2001) 19.

[13] J. A. Melero, G. D. Stucky, R. van Grieken, G. Morales, J. Mater. Chem. 12 (2002) 1664.

[14] J. A. Melero, R. van Grieken, G. Morales, Chem. Rev. 106 (2006) 3790.

[15] G.L. Athens, Y. Ein-Eli, B.F. Chmelka, Adv. Mater.19 (18) (2007) 2580.

[16] M. Alvaro, A. Corma, D. Das, V. Fornés, H. García, Chem. Commun. (2004) 956.

[17] D. J. Macquarrie, S. J. Tavener, M. A. Harmer, Chem. Commun. (2005) 2363.

[18] I. Díaz, C. Márquez-Alvárez, F. Mohino, J. Pérez-Pariente, E. Sastre, J. Catal. 193 (2000) 283.

[19] W.D. Bossaert, D. E. De Vos, W.M. Van Rhijn, J. Bullen, P.J. Grobet, P.A. Jacobs, J. Catal. 182 (1999) 156.

[20] I. Díaz, C. Márquez-Alvárez, F. Mohino, J. Pérez-Pariente, E. Sastre, J. Catal. 193 (2000) 295.

[21] J. A. Melero, R. van Grieken, G. Morales, M. Paniagua, Energy & Fuels 21 (2007) 1782.

[22] D. Das, J. F. Lee, S. Cheng, J. Catal. 223 (2004) 152.

[23] K. Wilson, A. F. Fee, D. J. Macquarrie, J.H. Clark, Appl. Catal. A: Gen. 228 (2002) 127.

[24] J. G. C. Shen, R. G. Herman, K. Klier, J. Phys. Chem. 106 (2002) 9975

[25] R. van Grieken, J. A. Melero, G. Morales, Appl. Catal. A: Gen. 289 (2005) 143

[26] X. Wang, C. C. Che, S. Y. Chen, Y. Mou, S. Cheng, Appl. Catal. 281 (2005) 47.

[27] B. Rác, A. Molnár, P. Forgo, M. Mohai, I. Bertoti, J. Mol. Catal. A: Chem 244 (2006) 46.

[28] J. A. Melero, R. van Grieken, G. Morales, V. Nuño, Catal. Commun. 5 (2004) 131.

[29] I.K. Mbaraka, B. H. Shanks, J. Am. Oil Chem. Soc. 83 (2006) 79.

[30] J. A. Bootsma, B. H. Shanks, Appl. Catal. A: Gen. 327 (2007) 44.

[31] Q. Yang, M. P. Kapoor, S. Inagaki, J. Am. Chem. Soc. 124 (2002) 9694.

[32] M. P. Kapoor, Q. Yang, Y. Goto, S Inagaki, Chem. Lett. 32 (2003) 914.

[33] S. Hamoudi, S. Royer, S. Kaliaguine, Microporous Mesoporous Mater. 71 (2004) 17.

[34] X. Yuan, H. I. Lee, J. W. Kim, J. E. Yie, J. M. Kim, Chem. Lett. 32 (2003) 650.

[35] Q. Yang, M.P. Kapoor, N. Shirokura, M. Ohashi, S. Inagaki, J. N. Kondo, K.J. Domen, J. Mater. Chem. 15 (2005) 666.

[36] B. Show, S. Hamoudi, M. H. Zahedi-Niaki, S. Kaliaguine, Microporous Mesoporous Mater. 79 (2005) 129.

[37] P.L. Dhepe, M. Ohashi, S. Inagaki, M. Ichikawa, A. Fukuoka, Catal. Lett. 102 (3-4) (2005) 163.

[38] J. D. Epping, B. F. Chmelka, Curr. Opin. Colloid In. 11 (2006) 81.

[39] J. Trebosc, J.W. Wiench, S. Huh, V. S. Y. Lin, M. Pruski, J. Am. Chem. Soc. 127 (2005) 7587.

[40] M. J. Duer, Introduction to Solid-State NMR Spectroscopy, Blackwell Publishing: Oxford, 2004.

[41] R. R. Ernst, G. Bodenhausen, A. Wokaun, Principles of Nuclear Magnetic Resonance in One and Two Dimensions, Oxford University Press: New York, 1997

[42] D. Zhao, Q. Huo, J. Feng, B. F. Chmelka, G. D. Stucky, J. Am. Chem. Soc. 120 (1998) 6024.

[43] P. T. Tanev, T. J. Pinnavaia, Science 267 (1999) 865.

[44] S. A. Bagshaw, E. Prouzet, T. J. Pinnavaia, Science 269 (1999) 1242.

[45] O. Muth, C. Schellbach, M. Fröba, Chem. Commun. (2001) 2032.

[46] H. Zhu, D. J. Jones, J. Zajac, J. Roziere, R. Dutartre, Chem. Commun. (2001) 2568.

[47] R. van Grieken, J. A. Melero, G. Morales, J. Mol. Catal. A: Chem. 256 (2006) 29.

[48] K. Shimizu, E. Hayashi, T. Hatamachi, T. Kodama, T. Higuchi, A. Satsuma, Y. Kitayama, J. Catal. 231 (2005) 131.